ChemComm

COMMUNICATION

View Article Online
View Journal | View Issue

Cite this: *Chem. Commun.*, 2023, **59**, 11256

Received 19th June 2023,
Accepted 10th August 2023

DOI: 10.1039/d3cc02922k

rsc.li/chemcomm

Highly efficient light-driven hydrogen evolution utilizing porphyrin-based nanoparticles†

Vasilis Nikolaou, ‡[a] Eleni Agapaki, ‡[a] Emmanouil Nikoloudakis, [a] Katerina Achilleos,[a] Kalliopi Ladomenou, [b] Georgios Charalambidis, [a] Evitina Triantafyllou [a] and Athanassios G. Coutsolelos *[ac]

We developed dye-sensitized photocatalytic systems (DSPs) by utilizing porphyrins as a photosensitizer (PS) or as a photosensitizer–catalyst (PS/CAT) upon their chemisorption onto platinum-doped titanium dioxide nanoparticles (Pt-TiO_2 NPs). The DSPs coated with Pt-Tc_3CP (PS/CAT entity) exhibited a record-high stability (25 500 TONs) and H_2 evolution activity (707 mmol g^{-1} h^{-1}) compared to similar DSPs in the literature.

The prolonged and continuous utilization of fossil fuels as primary energy sources generated significant environmental complications, since their combustion is responsible for the exponential increase of greenhouse gas emissions.[1] Hence, it is of great importance to establish cost-competitive, low-carbon technologies aiming to develop sustainable systems based on renewable sources.[2] Green hydrogen (H_2) besides being a clean fuel is a chemical feedstock as well, which can be imperative for accomplishing multi-sector decarbonization.[3] Light-driven H_2 production is an auspicious method because an abundant and clean energy (solar) is used to achieve an energy-rich storable compound (H_2) that can be used as a fuel.[4]

An efficient and facile approach toward light-driven H_2 evolution is the development of dye-sensitized photocatalytic systems (DSPs). Indeed, DSPs have received considerable attention recently due to their durability and tunability.[5,6] In such photocatalytic schemes, a photosensitizer (PS) and a catalyst (CAT) are immobilized onto titanium dioxide nanoparticles (TiO_2 NPs) forming a heterogeneous photocatalyst. Using a light source, the PS absorbs photons and gets excited; subsequently, electrons are injected into the conduction band of TiO_2. Finally, this flow of electrons reaches the CAT, which performs the reduction of H^+ to H_2 and the oxidized PS is regenerated using a sacrificial electron donor (SED).

A great number of different photosensitizers (PSs) and catalysts (CATs) have been utilized in TiO_2-based DSPs over the last decade (Fig. 1a).[6,7] In addition, by simply exchanging a molecular CAT with highly efficient Pt, researchers were able to develop schemes with greater stability and higher H_2 evolution activity (Fig. 1b).[8,9] There are various examples of porphyrinoids being utilized either as the PS or as the CAT in photocatalytic H_2 evolution, mainly due to their straightforward structural modification, which enables them to adopt desirable chemical and physical properties.[10,11] In spite of this fact though, only recently, our research group demonstrated a different approach (Fig. 1c), in which a single porphyrin (PS/CAT) was able to act as the light harvester and simultaneously as the catalyst.[12] Thus, in this approach, there is only one component (PS/CAT) that drives the photocatalytic H_2 evolution. Moving one step forward, herein we introduce an alternative approach, in which a PS/CAT derivative (a light harvester and a catalyst) is incorporated into Pt-TiO_2 NPs. The Pt-TiO_2 NPs act as a scaffold for the successful self-organization of the PS/CAT entities, an electron transport medium, and also as an additional photocatalyst. Thus, we combined metalated-porphyrin carboxylic acid derivatives with Pt-TiO_2 NPs and successfully developed highly efficient DSPs for H_2 evolution in aqueous media (Fig. 1d).

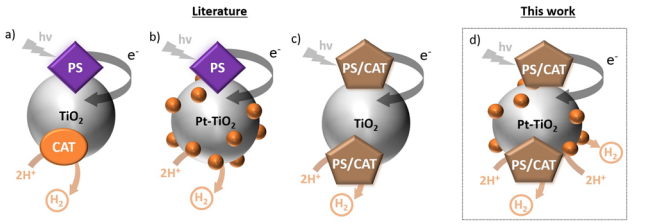

Fig. 1 The three established approaches in the literature to design DSPs for H_2 evolution: (a) PS and CAT on TiO_2 NPs, (b) PS onto $PtTiO_2$ NPs, and (c) PS–CAT onto TiO_2 NPs. (d) New approach: PS–CAT onto Pt-TiO_2 NPs.

[a] *Laboratory of Bioinorganic Chemistry, Department of Chemistry, University of Crete, Voutes Campus, 70013 Heraklion, Crete, Greece. E-mail: acoutsol@uoc.gr*
[b] *Laboratory of Inorganic Chemistry, Department of Chemistry, International Hellenic University, 65404 Kavala, Greece*
[c] *Institute of Electronic Structure and Laser (IESL) Foundation for Research and Technology - Hellas (FORTH), Vassilika Vouton, 70013 Heraklion, Crete, Greece*

† Electronic supplementary information (ESI) available: Experimental section, synthesis and characterization, adsorption studies and photocatalysis details. See DOI: https://doi.org/10.1039/d3cc02922k

‡ These authors have contributed equally.

We prepared two series of porphyrin derivatives metalated with zinc (Zn), palladium (Pd), and platinum (Pt) and introduced carboxylic acid units at their periphery as anchoring groups for their successful attachment onto Pt-TiO_2 NPs. As illustrated in Fig. S1 (ESI†), the carboxylic acid units were introduced either on a three-carbon alkyl chain (c_3) at the *para*-position of the phenyl ring (for the **M-T*c*$_3$CP** porphyrins) or at the *para*-position of the phenyl ring (for the derivatives **M-TCP**). The leading reasons to specifically modify these porphyrinoids in such a manner were derived from the results of our previous investigations.[12] Namely, **Pd-T*c*$_3$CP** and **Pt-T*c*$_3$CP** were able to self-organize onto TiO_2 NPs acting as both the PS and the CAT. In stark contrast, **Zn-T*c*$_3$CP** acted only as the PS, and as expected it did not produce any H_2. Although these DSPs demonstrated great stability and efficiency, the best conditions for H_2 evolution should be an organic/aqueous solvent mixture with 15% of triethanolamine as the SED. Thus, to explore their catalytic properties onto Pt-TiO_2 DSPs, we prepared three metalated **M-T*c*$_3$CP** (with Zn, Pd, and Pt, Fig. S1, ESI†) together with their respective **M-TCP** derivatives. More importantly, all these porphyrin-based Pt-TiO_2 DSPs operate in aqueous medium, rendering them as "greener" DSPs compared to the previous ones.[12]

The synthesis of **M-T*c*$_3$CP** was carried out following the procedures reported in the literature,[12–14] whereas **M-TCP** derivatives were prepared according to the synthetic approach described in detail in the ESI† (Scheme S1 and Fig. S2–S13). The absorption spectra of **M-TCP** and **M-T*c*$_3$CP** in freshly distilled toluene/ethanol solutions (ratio 1 : 1) are illustrated in Fig. 2. Their absorption coefficient numbers and their absorption data (λ_{max} of Soret and Q bands) are listed in Table S1 (ESI†). In all cases, typical absorption features for such metalated porphyrinoids[15] are observed. The electrochemical properties of all **M-T*c*$_3$Ps** were investigated by means of cyclic voltammetry (Table S2, ESI†). The driving force regarding the electron injection from the porphyrins to TiO_2 (ΔG_{inj}), as well as their regeneration from the SED (ΔG_{reg}) indicate that both processes are thermodynamically favorable (see the ESI† for details; Table S2).

The initial step for the light-driven H_2 evolution experiment is the chemisorption of the complexes onto the Pt-TiO_2 NPs. Various initial concentrations of metalated porphyrins were utilized in order to optimize the chemisorption of the porphyrins onto Pt-TiO_2 NPs (see the ESI†). All the absorption spectra before and after their chemisorption are available in the ESI† (Fig. S14–S16) and the respective dye loadings (DLs) for each complex are listed in Tables S3–S8 (ESI†). In Fig. 2c, the absorption spectra of **Pt-T*c*$_3$CP** before and after chemisorption onto Pt-TiO_2 NPs are presented. It is worth noting that by using this initial concentration (*viz.* 1.0×10^{-5} M), a quantitative loading of the porphyrin (DL = 100%) was achieved in all different cases.

In a typical H_2 evolution experiment, 5 mg of the porphyrin-sensitized Pt-TiO_2 NPs were dispersed in an aqueous solution (see the ESI† for details). The dispersions were prepared in a glass vial, sealed with a rubber septum, and irradiated using a 40 W light-emitting diode lamp (LED lamp, Fig. S17, ESI†). Upon photo-irradiation, all different metalated porphyrins (**M-TCP** and **M-T*c*$_3$CP**) demonstrated H_2 production. The photocatalytic activity of the porphyrin-based DSPs was strongly dependent on the amount of the adsorbed porphyrin onto the TiO_2 NPs (Tables S2–S7, ESI†). By considering the best photocatalytic data for each DSP (Table 1), we can safely conclude that all the **M-T*c*$_3$TCP** derivatives outperform their respective **M-TCP** ones, in terms of both stability (TONs) and efficiency (total H_2 evolution, mmol g^{-1} h^{-1}). Nevertheless, **Zn-TCP** and **Zn-T*c*$_3$TCP** demonstrated almost identical TONs ($\sim$1100) and nearly the same amount of H_2 evolution ($\sim$400 mmol g^{-1} h^{-1}). This indicates that the photocatalytic activity of Zn–porphyrin derivatives is not affected by the different anchoring groups (the rigid carboxylic acid group *vs.* flexible c_3-carboxylic acid), confirming their sole role as PSs.

In contrast, both **Pd-T*c*$_3$TCP** and **Pt-T*c*$_3$TCP** exhibited superior TONs and H_2 evolution rates compared to their counterparts **Pd-TCP** and **Pt-TCP**, respectively (Table 1). More specifically, **Pd-T*c*$_3$CP** achieved 7722 TONs and 593 mmol g^{-1} h^{-1} of H_2 evolution, the values of which are significantly greater than those of **Pd-TCP** (1147 TONs and 256 mmol g^{-1} h^{-1} of H_2, respectively). In a similar manner, nonetheless reaching even greater results, **Pt-T*c*$_3$CP** demonstrated 11 607 TONs and 458 mmol g^{-1} h^{-1} of H_2 evolution, outperforming **Pt-TCP** (2525 TONs and 378 mmol g^{-1} h^{-1} of H_2). A possible explanation for the enhanced performance of the **M-T*c*$_3$CP** derivatives compared to that of the **M-TCP** ones is that the adsorption *via* four anchoring groups leads to a well-oriented self-organization of the **M-T*c*$_3$CPs**. This was indeed verified by scanning electron microscopy (SEM) experiments, which demonstrated that **Pt-T*c*$_3$P** undergoes a well-oriented self-organization in spherical nanostructures (Fig. S18b, ESI†). In contrast, both **Zn-TCP** (Fig. S18c, ESI†) and **Pt-TCP** (Fig. S18d, ESI†) self-aggregate

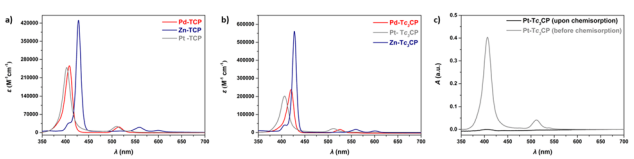

Fig. 2 Extinction coefficient (ε) of (a) **M-TCP** and (b) **M-*c*$_3$TCP** derivatives (M: Zn, Pd, or Pt) in freshly distilled toluene/ethanol (1 : 1 ratio) solutions. (c) Absorption spectra of **Pt-Tc$_3$CP** (1.0×10^{-5} M) before and after chemisorption onto Pt-TiO_2 NPs.

Table 1 The best photocatalytic data for each porphyrin-based DSP are listed below

Porphyrin	TONs *vs.* PS[a]	TONs *vs.* CAT[b]	H_2 evolution rate[c]
Zn-TCP	1192	1686	360
Zn-T*c*$_3$CP	1031	1972	421
Pd-TCP	1147	814	256
Pd-T*c*$_3$CP	7722	2097	593
Pt-TCP	2525	1772	378
Pt-T*c*$_3$CP	11 607	1216	707

[a] TON in 24 hours *vs.* PS = porphyrin (see the ESI for details). [b] TON in 24 hours *vs.* CAT. In the cases of **Zn-TCP** and **Zn-T*c*$_3$CP**: CAT = $PtTiO_2$. However, in the cases of **Pd-TCP**, **Pd-T*c*$_3$CP**, **Pt-TCP**, and **Pt-T*c*$_3$CP**: CAT = $PtTiO_2$ and Pt- or Pd-porphyrin (see the ESI for details). [c] H_2 evolution rate (mmol g^{-1} h^{-1}) *vs.* total g of CAT in 24 hours (see the ESI for details).

on the top of the spherical Pt-TiO2 NPs (Fig. S18a, ESI†) In addition, the strong binding of **Pt-T*c*$_3$CP** is illustrated in Fig. S19 (ESI†), since the peaks correlated with the ν(C=O) and the ν(C–O) stretching of the unbound carboxylic acid group at ~1700 and 1200 cm^{-1}, respectively disappeared in the FT-IR spectrum of the chemisorbed sample (**Pt-T*c*$_3$CP@Pt-TiO$_2$**). In perfect agreement with our recent report, these catalytic results underline again the diverse behavior of both Pd- and Pt-porphyrins acting as PS/CAT entities, in contrast to the respective Zn-porphyrins, which act as PSs.[12]

In an effort to provide an even more fair assessment for the porphyrin-based DSPs developed herein, we explored their catalytic activity under the same dye loading (DL = 100%) by utilizing initial porphyrin solutions of 1.0×10^{-5} M in all cases (see Tables S3–S8, ESI†). As illustrated in Fig. 3, **Pt-T*c*$_3$CP** and **Pd-T*c*$_3$CP** reached 10 819 and 7722 TONs and H_2 evolution rates of 707 and 342 mmol g^{-1} h^{-1}, respectively, outperforming their **M-TCP** counterparts and the respective Zn-porphyrinoinds. Similar to the behavior during the best performing photovoltaic experiments (Table 1), using these DSPs (with DL = 100%), the photocatalytic response of **Zn-T*c*$_3$CP** and **Zn-TCP** was yet again almost identical (~1100 TONs and ~50 mmol g^{-1} h^{-1} of H_2). Furthermore, by comparing the **M-TCP** derivatives, evidently **Pt-TCP** (2018 TONs and 82 mmol g^{-1} h^{-1} of H_2) is a better photocatalyst compared to **Pd-TCP** (1096 TONs and 49 mmol g^{-1} h^{-1} of H_2). It may be well argued that **Pd-TCP** acts as a photosensitizer in this case, since the photocatalytic values are almost the same as the Zn–porphyrin-based DSPs (~1100 TONs and ~50 mmol g^{-1} h^{-1} of H_2). In contrast, **Pt-TCP** reached almost double values concerning the TONs and the H_2 evolution rates (2018 TONs and 82 mmol g^{-1} h^{-1}, respectively) emphasizing once more the PS/CAT nature of the Pt–porphyrin-based DSPs.[12]

To evaluate the stability of our best performing system (**Pt-T*c*$_3$CP@PtTiO$_2$**), we performed long-term photocatalytic experiments. As illustrated in Fig. S20a (ESI†), the DSPs coated with **Pt-T*c*$_3$CP** exhibited great stability reaching 25 500 TONs, and high H_2 evolution activity (316 mmol g^{-1} h^{-1} of H_2). Upon 48 h of continuous visible light irradiation, the H_2 evolution was stopped and the DSPs reached a plateau. In an effort to investigate the reason for deactivation, in four different experiments, we added either (a) **Pt-T*c*$_3$CP**, (b) AA 1M, (c) Pt-TiO$_2$, or (d) **Pt-T*c*$_3$CP@Pt-TiO$_2$**; however, we did not observe any reactivation of the H_2 production (Fig. S20b, ESI†). Only when both the photocatalytic NPs (**Pt-T*c*$_3$CP@Pt-TiO$_2$**) and the SED (AA) were added, H_2 production was detected. These experiments demonstrate that both the SED and the **Pt-T*c*$_3$CP@Pt-TiO$_2$** photocatalyst have been converted into non-active compounds/materials. Indeed, the absorption spectrum of the SED before and after the catalytic experiment significantly changes (Fig. S20c, ESI†). In contrast, the SEM experiments demonstrated that the morphology of Pt-TiO$_2$ is not affected at all upon photocatalysis (Fig. S21, ESI†). More specifically, similar to our previous study,[19] **Pt-T*c*$_3$CP** exhibits a spherical self-organization on the Pt-TiO$_2$ NPs which is retained even upon the 48 h of photocatalysis. Hence, we concluded that the deactivation of the **Pt-T*c*$_3$CP@Pt-TiO$_2$** system can be attributed to the degradation of the porphyrin and the SED, rendering them the limiting factors of our DSPs.

In addition, we evaluated the correlation between the amount of porphyrin and the H_2 evolution rate for all **M-T*c*$_3$CP** and **M-TCP** (M: Zn, Pt, and Pd, Fig. S22, ESI†). Interestingly, for all **M-TCP** porphyrins and **Zn-T*c*$_3$CP,** a linear correlation between the amount of the porphyrin and the H_2 evolution rate is observed. In particular, in all cases, the higher H_2 evolution rate was detected for the greater porphyrin quantity (~ 3.0×10^{-7} mol). In stark contrast, the respective experiments for **Pt-T*c*$_3$CP** and **Pd-T*c*$_3$CP** revealed that the highest H_2 production rate is not associated with the greater amount of the porphyrin. In the case of **Pd-T*c*$_3$CP,** the highest H_2 production rate of 1.5×10^{-7} mol was detected, whereas for the **Pt-T*c*$_3$CP** it was 3.0×10^{-8} mol of the porphyrin. These findings confirm once more the hypothesis that the enhanced catalytic efficiency of **Pt-T*c*$_3$CP** and **Pd-T*c*$_3$CP** can be accredited to the well-oriented self-organization of the porphyrinoids on the surface of the Pt-TiO$_2$ performing as PS/CAT entities.

To sum up, we demonstrated that dispersion of porphyrin-based DSPs in an aqueous medium is an auspicious method to develop highly performing photocatalytic nanoparticles. Unlike the reported research works to date, the utilized porphyrins herein are able to act at the same time as a light harvester and a catalyst (PS/CAT). Hence, we introduced a more facile – in terms of preparation protocols – approach, compared to more complex structures (PS-dyads) or a combination of two entities (PS + CAT) that were reported in other studies.[9–13,16–21] We prepared different metalated tetra-carboxylic acid porphyrins to explore the impact of two significant factors: (i) the different metals and (ii) the position of the anchoring group in light-driven H_2 production. Interestingly, in contrast to Pd- and Pt-porphyrins, the catalytic properties of the respective Zn-porphyrins were not affected by the different anchoring groups. It is worth mentioning that the different positioning of the anchoring groups strongly impacted the H_2 evolution of both Pd- and Pt-porphyrin-based DSPs. We can safely assume that the **M-TCP** derivatives use maximum two carboxylic acids to

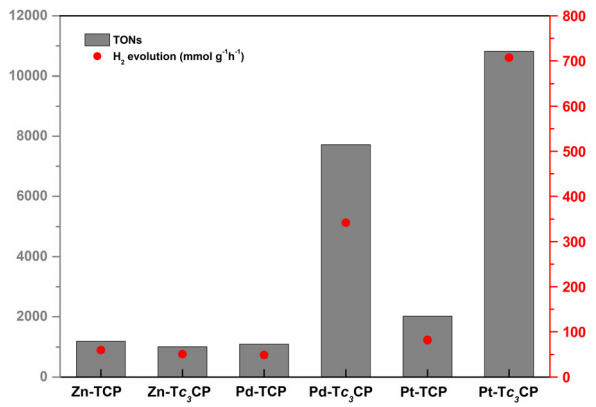

Fig. 3 Comparison of all the **M-TCP** and **M-*c*$_3$TCP** derivatives (M: Zn, Pd, or Pt) concerning their catalytic activity (TONs and H_2 evolution rates). In all cases, the concentration of the initial porphyrin solution used for the chemisorption of the porphyrin was 1.0×10^{-5} M and the resulting dye-loading percentage was DL = 100%.

Table 2 Comparison between the best porphyrin-based DSPs in the literature and this work. In all the reports below, a porphyrinoid (or a porphyrin-based dyad) was utilized as the PS, Pt-TiO_2 NPs as the catalysts, and an aqueous solution as the solvent

PS	SED	TONs	Irr. time	H_2 evolution[b]	Publication
Pt-T*c*$_3$CP	AA (1M)	25 500[a]	24/48	707	This work
YD2-*o*-C8	AA (0.5M)	11 900	120	272	28
BDP-Por-BDP(Im)	AA (1M)	18 600	72	225	31
ZnP-dyad	AA (0.5M)	12 800	120	173	28
LGtT	TEOA 20%	14 792	5	7.4	29
LG-DtT	TEOA 20%	13 282	5	6.7	29
LG-5	TEOA 20%	6582	5	3.3	29
PdTHPP	TEOA 10%	158	5	2.0	30
ZnTHPP	TEOA 10%	92	5	1.3	30
THPP	TEOA 10%	39	5	0.6	30
SnTPyP	EDTA	7.5	4	0.2	27
Sn(IV)TCPP	C_6H_{12}[c]	—	5	0.5[d]	26

[a] TON in 48 hours *vs.* PS = porphyrin (see the ESI for details). [b] H_2 evolution rate (mmol g^{-1} h^{-1}) *vs.* total g of CAT in 24 hours. CAT = $PtTiO_2$ and Pt-T*c*$_3$CP (see the ESI for details). [c] The oxygenation of cyclohexene (C_6H_{12}) was studied instead of the presence of a SED. [d] In μmol g^{-1} h^{-1}.

bound onto the NPs, whereas the chemisorption of **M-T*c*$_3$CP** can be achieved *via* four carboxylic acids.[22–25] This multisided anchoring mode of **M-T*c*$_3$CP** derivatives resulted in their enhanced photocatalytic activity (Table 1).

In Table 2, a thorough comparison between our work and the highest performing porphyrin-based DSPs in the literature is given. In all these reports, a porphyrinoid or a porphyrin-based dyad was utilized as the PS and Pt-TiO_2 NPs as the catalyst entity, and the photocatalytic reaction was performed in an aqueous solvent. Remarkably, the H_2 evolution rate of our DSPs developed with **Pt-T*c*$_3$CP** is more than two times greater (707 mmol g^{-1} h^{-1}) compared to other porphyrin-based DSPs reported in the literature (Table 1). In addition, besides the high efficiency, the developed DSPs herein exhibited a greater stability as well, reaching 25 500 TONs. Overall, we showed stable and efficient DSPs for H_2 evolution by utilizing PS–CAT derivatives in aqueous media. In the future, several aspects should be explored targeting the development of earth-abundant dispersions with high stability and efficiency.

This research was financed by the European Union and Greek national funds through the Operational Program Competitiveness, Entrepreneurship, and Innovation, under the call RESEARCH-CREATE-INNOVATE (project code: T1EDK-01504). In addition, this research has been co-financed by the European Union and Greek national funds through the Regional Operational Program "Crete 2014-2020," project code OPS:5029187. Moreover, the European Commission's Seventh Framework Program (FP7/2007-2013) under grant agreement no. 229927 (FP7-REGPOT-2008-1, Project BIO-SOLENUTI) and the Special Research Account of the University of Crete are gratefully acknowledged for the financial support of this research.

Conflicts of interest

There are no conflicts to declare.

Notes and references

1 J. Du, D. Xiang, K. Zhou, L. Wang, J. Yu, H. Xia, L. Zhao, H. Liu and W. Zhou, *Nano Energy*, 2022, **104**, 107875.
2 A. Rahman, O. Farrok and M. M. Haque, *Renewable Sustainable Energy Rev.*, 2022, **161**, 112279.
3 S. Martinez-Villarreal, M. Kammoun and A. Richel, *Curr. Opin. Green Sustainable Chem.*, 2023, **39**, 100716.
4 J. Radhakrishnan, S. Ratna and K. Biswas, *Inorg. Chem. Commun.*, 2022, **145**, 109971.
5 G. Reginato, L. Zani, M. Calamante, A. Mordini and A. Dessì, *Eur. J. Inorg. Chem.*, 2020, 899–917.
6 J. Willkomm, K. L. Orchard, A. Reynal, E. Pastor, J. R. Durrant and E. Reisner, *Chem. Soc. Rev.*, 2016, **45**, 9–23.
7 S. Rajak, N.-N. Vu, P. Kaur, A. Duong and P. Nguyen-Tri, *Coord. Chem. Rev.*, 2022, **456**, 214375.
8 L. Zani, M. Melchionna, T. Montini and P. Fornasiero, *J. Phys.: Energy*, 2021, **3**, 031001.
9 J.-F. Huang, Y. Lei, T. Luo and J.-M. Liu, *ChemSusChem*, 2020, **13**, 5863–5895.
10 E. Nikoloudakis, I. López-Duarte, G. Charalambidis, K. Ladomenou, M. Ince and A. G. Coutsolelos, *Chem. Soc. Rev.*, 2022, **51**, 6965–7045.
11 J. S. O'Neill, L. Kearney, M. P. Brandon and M. T. Pryce, *Coord. Chem. Rev.*, 2022, **467**, 214599.
12 V. Nikolaou, G. Charalambidis, K. Ladomenou, E. Nikoloudakis, C. Drivas, I. Vamvasakis, S. Panagiotakis, G. Landrou, E. Agapaki, C. Stangel, C. Henkel, J. Joseph, G. Armatas, M. Vasilopoulou, S. Kennou, D. M. Guldi and A. G. Coutsolelos, *ChemSusChem*, 2021, **14**, 961–970.
13 I. D. Kostas, A. G. Coutsolelos, G. Charalambidis and A. Skondra, *Tetrahedron Lett.*, 2007, **48**, 6688–6691.
14 C. Stangel, D. Daphnomili, T. Lazarides, M. Drev, U. O. Krasovec and A. G. Coutsolelos, *Polyhedron*, 2013, **52**, 1016–1023.
15 K. T. Weber, K. Karikis, M. D. Weber, P. B. Coto, A. Charisiadis, D. Charitaki, G. Charalambidis, P. Angaridis, A. G. Coutsolelos and R. D. Costa, *Dalton Trans.*, 2016, **45**, 13284–13288.
16 K. Kurimoto, T. Yamazaki, Y. Suzuri, Y. Nabetani, S. Onuki, S. Takagi, T. Shimada, H. Tachibana and H. Inoue, *Photochem. Photobiol. Sci.*, 2014, **13**, 154–156.
17 E. Koposova, X. Liu, A. Pendin, B. Thiele, G. Shumilova, Y. Ermolenko, A. Offenhäusser and Y. Mourzina, *J. Phys. Chem. C*, 2016, **120**, 13873–13890.
18 P.-Y. Ho, M. F. Mark, Y. Wang, S.-C. Yiu, W.-H. Yu, C.-L. Ho, D. W. McCamant, R. Eisenberg and S. Huang, *ChemSusChem*, 2018, **11**, 2517–2528.
19 P. S. Gangadhar, S. Gonuguntla, S. Madanaboina, N. Islavath, U. Pal and L. Giribabu, *J. Photochem. Photobiol., A*, 2020, **392**, 112408.
20 L. Y. Huang, J. F. Huang, Y. Lei, S. Qin and J. M. Liu, *Catalysts*, 2020, **10**(6), 656.
21 V. Nikolaou, G. Charalambidis, G. Landrou, E. Nikoloudakis, A. Planchat, R. Tsalameni, K. Junghans, A. Kahnt, F. Odobel and A. G. Coutsolelos, *Acs Appl. Energy Mater.*, 2021, **4**, 10042–10049.
22 A. S. Hart, C. B. Kc, H. B. Gobeze, L. R. Sequeira and F. D'Souza, *ACS Appl. Mater. Interfaces*, 2013, **5**, 5314–5323.
23 L. Zhang and J. M. Cole, *ACS Appl. Mater. Interfaces*, 2015, **7**, 3427–3455.
24 K. Ladomenou, T. N. Kitsopoulos, G. D. Sharma and A. G. Coutsolelos, *Rsc Adv.*, 2014, **4**, 21379–21404.
25 J. Rochford, D. Chu, A. Hagfeldt and E. Galoppini, *J. Am. Chem. Soc.*, 2007, **129**, 4655–4665.
26 K. Kurimoto, T. Yamazaki, Y. Suzuri, Y. Nabetani, S. Onuki, S. Takagi, T. Shimada, H. Tachibana and H. Inoue, *Photochem. Photobiol. Sci.*, 2014, **13**, 154–156.
27 E. Koposova, X. Liu, A. Pendin, B. Thiele, G. Shumilova, Y. Ermolenko, A. Offenhäusser and Y. Mourzina, *J. Phys. Chem. C*, 2016, **120**, 13873–13890.
28 P.-Y. Ho, M. F. Mark, Y. Wang, S.-C. Yiu, W.-H. Yu, C.-L. Ho, D. W. McCamant, R. Eisenberg and S. Huang, *ChemSusChem*, 2018, **11**, 2517–2528.
29 P. S. Gangadhar, S. Gonuguntla, S. Madanaboina, N. Islavath, U. Pal and L. Giribabu, *J. Photochem. Photobiol., A*, 2020, **392**, 112408.
30 L. Y. Huang, J. F. Huang, Y. Lei, S. Qin and J. M. Liu, *Catalysts*, 2020, **10**, 656.
31 V. Nikolaou, G. Charalambidis, G. Landrou, E. Nikoloudakis, A. Planchat, R. Tsalameni, K. Junghans, A. Kahnt, F. Odobel and A. G. Coutsolelos, *ACS Appl. Energy Mater.*, 2021, **4**, 10042–10049.